View metadata, citation and similar papers at core.ac.uk
brought to you by CORE
provided by The University of Utah: J. Willard Marriott Digital Library

PHYSICAL REVIEW B **86**, 115442 (2012)

# Resonant finite-size impurities in graphene, unitary limit, and Friedel oscillations

V. V. Mkhitaryan* and E. G. Mishchenko
*Department of Physics and Astronomy, University of Utah, Salt Lake City, Utah 84112, USA*
(Received 21 June 2012; published 25 September 2012)

A unitary limit for model point scatterers in graphene is known to reveal low-energy resonances. The same limit could be achieved from hybridization of band electrons with the localized impurity level positioned in the vicinity of the Fermi level. The finite-size defects represent an easier realization of the effective unitary limit, occurring when the Fermi wavelength induced by the potential becomes of the order of the size of the defect. We calculate the induced electron density and find two signatures of a strong impurity, independent of its specific realization. The dependence of the impurity-induced electron density on the distance changes near resonances from $\propto r^{-3}$ to $\propto r^{-2}$. The total number of induced particles at the resonance is equal to one per degree of spin and valley degeneracy. The effects of doping on the induced density are found.

DOI: 10.1103/PhysRevB.86.115442 PACS number(s): 73.22.Pr, 73.20.At, 73.22.Dj

## I. INTRODUCTION

In conventional three-dimensional electron systems probe charges are screened exponentially with the distance.[1] In degenerate metals at distances exceeding the screening radius the nonmonotonic power-law tail develops, $\propto \cos(2k_F r)/r^3$, that originates from electron backscattering with the change of momentum equal to $2k_F$, twice the Fermi momentum.[2] Correspondingly, in a conventional two-dimensional electron gas[3] the amplitude of these Friedel oscillations decays as only the second power of the distance $\propto r^{-2}$. In systems with the Berry phase and nontrivial chiral spectrum, Friedel oscillations could still decay faster, $\propto r^{-3}$, if the states with momenta $\mathbf{k}$ and $-\mathbf{k}$ are orthogonal and backscattering is suppressed.[4] In particular, this happens in the case of doped graphene,[5] when the Fermi level is shifted away from the Dirac points, $k_F \neq 0$, with pseudospin-diagonal impurity potential. For a short-range impurity with the potential $V(\mathbf{r}) = U\delta(\mathbf{r})$ the resulting induced electron density is[6,7] (we use units with $\hbar = 1$)

$$n(\mathbf{r}) = \frac{U}{2\pi^2 v r^3}\cos(2k_F r), \quad k_F r \gg 1, \tag{1}$$

where $v$ is the velocity of Dirac electrons. Within the linear response approximation the derivation of this result is straightforward with the help of the density-density correlation function $\Pi_\omega(\mathbf{r}-\mathbf{r}')$ taken in the static $\omega = 0$ limit: $n = \Pi_0 \otimes V$. In the case of a short-range potential the latter formula gives simply $n(\mathbf{r}) = U\Pi_0(\mathbf{r})$ and eventually leads to Eq. (1).

The calculation outlined above can be extended easily to the case of intrinsic graphene, $k_F = 0$, or, equivalently, to short distances, $r \ll k_F^{-1}$. Interestingly, the functional form (1) is recovered again, as can be verified within the same linear response approach; the only change is in the numerical factor $\pi/4$:

$$n(\mathbf{r}) = \frac{U}{8\pi v r^3}, \quad k_F r \ll 1. \tag{2}$$

The nonintegrable singularity at $r \to 0$ makes the total induced electron density $\int n(\mathbf{r})d^2r$ diverge as a power law. This indicates the failure of the first Born approximation when $U/vr \sim 1$. Fortunately, the $\delta$-function potential allows for an exact nonperturbative solution via the $T$ matrix in terms of the electron Green's function, $T(E) = U/[1 - U\sum_{\mathbf{p}} G(E,\mathbf{p})]$, which yields

$$T(E) = \frac{U}{1 + \frac{U}{2\pi v^2}E[\ln(v/a|E|) + i\pi/2]}. \tag{3}$$

The ultraviolet divergence is cut off at short distances of the order of the lattice spacing $a$.

In the "unitary limit" of strong interaction, $U \to \infty$, the resonant form of the $T$ matrix (3) clearly should lead to a significant modification of the dependence of the induced density on distance. It is not difficult to obtain a rough estimate for the effect: since typical energies are $|E| \sim v/r$, we immediately conclude that in the logarithmic approximation $n(r) \sim 1/[r^2 \ln(r/a)]$. Surprisingly, as we demonstrate in the present paper this crude guess is incorrect and the induced density in the unitary limit is in fact *suppressed* according to ($U > 0$)

$$n(r) = \frac{2}{\pi r^2 \ln(U/va)}. \tag{4}$$

The behavior described by Eq. (4) cannot be properly accounted for if the imaginary part of $T(E)$ is neglected. It turns out that, despite the imaginary part in the denominator of Eq. (3) being small compared with the logarithmically large real part, the two parts lead to the contributions that largely cancel each other.

The suppression of the local density (4) at the unitary limit does not mean that the *total* density vanishes too. Quite to the contrary, as the range of distances, $r \ll U/v$, where Eq. (4) is applicable increases with increasing $U$, the total induced density tends to a limit $\int n(\mathbf{r})d^2r \to 4$, i.e., *one electron* per spin/sublattice.

The resonant $1/E$ behavior of the scattering amplitude in graphene has significant implications. In particular, the unitary limit leads to singular corrections to the low-energy density of states.[8–10] The effective Casimir-like coupling between two point impurities (adatoms) is predicted to become long range in the unitary limit[11] with the potential energy $\propto [r\ln(r/a)]^{-1}$. However, achieving the unitary limit by the strength of the potential alone might be difficult. To illustrate this for atomic impurities let us consider the simplest microscopic model of a point impurity that yields expression (3), namely, the tight-binding approximation for the honeycomb lattice where

 ©2012 American Physical Society

a single carbon atom is substituted with an impurity atom.[12,13] In that case the effective strength of the $\delta$ function is simply $U \sim \langle V_i \rangle a^2$, where $a = 1.4$ Å is the interatomic distance and $\langle V_i \rangle$ is the expectation value of the impurity's potential energy (calculated with the help of the unperturbed orbital). We therefore estimate that for the unitary limit to be effectively achieved at distances $r$ the strength of the impurity should exceed

$$\langle V_i \rangle \gg t \frac{r/a}{\ln (r/a)}, \tag{5}$$

with $t = v/a \approx 3$ eV being the hopping energy. From expression (5) it follows that already at distances $r \sim 1$–$2$ nm the impurity strength $\langle V_i \rangle$ needs to be of the order of tens of eV, which is clearly impractical.

This restriction could be lifted if an impurity has a localized level with low energy $\varepsilon_0 \ll t$ leading to a resonant enhancement of scattering.[14] The limit of strong impurities could also be realized in vacancies.[15] Yet another possibility is a finite-size scatterer.[16,17] Indeed, consider an impurity potential of finite radius $\rho$. Treating potential energy perturbatively is justified as long as the characteristic potential energy $V_0$ is small compared with the typical kinetic energy, $v/\rho$. The latter estimate uses that the typical electron momenta inside the potential in *intrinsic* graphene are determined by the width of the potential, $k \sim 1/\rho$. The Born approximation, Eqs. (1) and (2), then holds true for small effective dimensionless coupling constants, $g = V_0 \rho / v \ll 1$. The nonperturbative regime is reached when $g \sim 1$, which is a *much less stringent* condition (by a factor $r/a$) than the above-discussed condition for a $\delta$-function impurity. This is also evident from the correspondence $\pi V_0 \rho^2 \to U$ expected to exist between the potentials at $\rho \to 0$.

In the present paper we address the response of Dirac electrons in graphene to strong impurities. Since the case of a finite-size scatterer reveals the richest behavior and is free from low-distance singularities, we are going to address it first. Still, the results obtained are applicable to other strong impurities with proper modifications. In Sec. II we begin by analyzing the square potential problem, $V(\mathbf{r}) = V_0 \Theta(\rho - r)$, and finding the induced density in the case of intrinsic graphene. The unitary limit is resonantly achieved whenever the coupling constant coincides with a zero of a Bessel function, $J_0(g) = 0$, where the induced density changes its dependence on the distance to $\propto 1/r^2$. Physically, resonances are related to the number of wavelengths induced by the potential $V_0$ that fit inside it. Such a possibility is absent for pointlike scatterers where the strength of the potential is the only variable parameter that has to be sent to infinity in order to achieve the unitary limit. In Sec. III we address the effects that occur due to finite Fermi momentum in doped graphene, including Friedel oscillations.

## II. IMPURITY-INDUCED ELECTRON DENSITY IN INTRINSIC GRAPHENE

Solutions of the Dirac equation in a centrally symmetric potential $V(r)$ have been considered extensively before,[13,16,18] but for the sake of convenience we present them here again. The Dirac equation

$$-iv \begin{pmatrix} 0 & \partial_x - i\partial_y \\ \partial_x + i\partial_y & 0 \end{pmatrix} \psi = [E - V(r)]\psi \tag{6}$$

determines the two-component wave function is a linear combination of partial waves with the angular momentum quantum number $m = \pm 1/2, \pm 3/2, \ldots,$

$$\psi_m = \frac{e^{im\phi}}{\sqrt{2\pi}} \begin{pmatrix} \varphi_1 e^{-i\phi/2} \\ \varphi_2 e^{i\phi/2} \end{pmatrix}. \tag{7}$$

Here we introduced the polar coordinates: $x + iy = re^{i\phi}$.

We first focus on the repulsive potential $V_0 > 0$. As the integral over all filled states (negative energies $E$) has to be taken eventually, we parametrize $E = -vk$ with positive $k$. Then the Schrödinger equation (6) gives two coupled equations for $r < \rho$,

$$\begin{aligned} \partial_r \varphi_1 - \frac{m - 1/2}{r} \varphi_1 &= -i \left( k + \frac{V_0}{v} \right) \varphi_2, \\ \partial_r \varphi_2 + \frac{m + 1/2}{r} \varphi_2 &= -i \left( k + \frac{V_0}{v} \right) \varphi_1. \end{aligned} \tag{8}$$

Similarly, for $r > \rho$ the wave functions obey the same equations as Eqs. (8) but without $V_0$. Both inside and outside of the potential the wave functions satisfying the condition of regularity at $r = 0$ are given in terms of Bessel functions,

$$\begin{pmatrix} \varphi_1 \\ \varphi_2 \end{pmatrix} = A \begin{pmatrix} J_{m-1/2}(kr + gr/\rho) \\ -i J_{m+1/2}(kr + gr/\rho) \end{pmatrix} \tag{9}$$

for $r < \rho$, and

$$B \begin{pmatrix} \mathrm{sgn}(k) J_{m-1/2}(|k|r) \\ -i J_{m+1/2}(|k|r) \end{pmatrix} + C \begin{pmatrix} \mathrm{sgn}(k) Y_{m-1/2}(|k|r) \\ -i Y_{m+1/2}(|k|r) \end{pmatrix} \tag{10}$$

for $r > \rho$. The coefficients $A$, $B$, and $C$ are found from the conditions of continuity at $r = \rho$. The normalized[19] wave functions for $m = 1/2$ in the outer region, $r > \rho$, are then found to be

$$\begin{aligned} \varphi_1 &= \mathrm{sgn}(k) \frac{\sqrt{\pi |k|}}{\sqrt{\beta^2 + \gamma^2}} [\beta J_0(|k|r) + \gamma Y_0(|k|r)], \\ \varphi_2 &= -i \frac{\sqrt{\pi |k|}}{\sqrt{\beta^2 + \gamma^2}} [\beta J_1(|k|r) + \gamma Y_1(|k|r)], \end{aligned} \tag{11}$$

where the following coefficients are defined ($k > 0$):

$$\begin{aligned} \beta &= J_1(k\rho + g) Y_0(k\rho) - J_0(k\rho + g) Y_1(k\rho), \\ \gamma &= J_0(k\rho + g) J_1(k\rho) - J_1(k\rho + g) J_0(k\rho). \end{aligned} \tag{12}$$

The electron density $n = \frac{2}{\pi^2} \int dk (|\varphi_1|^2 + |\varphi_2|^2)$ takes into account the contributions from the two leading channels with $m = \pm 1/2$ as well as spin/valley degeneracy. Subtracting the equilibrium ($g = 0$) density, we find

$$\begin{aligned} n(r) = \frac{2}{\pi} \sum_{i=0,1} \int_0^\infty \frac{dk\, k}{\beta^2 + \gamma^2} \big\{ & 2\beta\gamma\ J_i(kr) Y_i(kr) \\ & + \gamma^2 \big[ Y_i^2(kr) - J_i^2(kr) \big] \big\}. \end{aligned} \tag{13}$$

The latter equation can be written more compactly if we use the Hankel function, $H^{(1)}(z) = J(z) + iY(z)$, to obtain

$$n(r) = \frac{2}{\pi}\mathrm{Im}\sum_{i=0,1}\int_0^\infty \frac{dk\,k\gamma}{\beta + i\gamma}\left[H_i^{(1)}(kr)\right]^2. \quad (14)$$

We now analyze this expression for different values of the impurity strength $g$. The oscillating behavior of the Hankel functions ensures that the integral in Eq. (14) converges at $k \sim 1/r$. Since we are interested in the behavior at long distances $r \gg \rho$ we can write, for generic values of $g$ (though still $\gg \rho/r$),

$$\gamma \approx -J_1(g). \quad (15)$$

The latter approximation is valid unless $g$ is very close to a zero of the Bessel function $J_1(g)$ (see below). Similarly, by keeping the singular terms in the small-argument expansion of the Bessel functions we can write, for the second coefficient,

$$\beta \approx J_1(g)Y_0(k\rho) - J_0(g)Y_1(k\rho) \approx \frac{2}{\pi}\left[J_1(g)\ln(k\rho) + J_0(g)\frac{1}{k\rho}\right]. \quad (16)$$

Substituting approximate Eqs. (15) and (16) into the exact formula (14) we arrive at the induced density,

$$n(r) = \frac{1}{r^2}\mathrm{Im}\sum_{i=0,1}\int_0^\infty \frac{dz\,z\left[H_i^{(1)}(z)\right]^2}{\ln\left(\frac{r}{\rho z}\right) - \frac{J_0(g)}{J_1(g)}\frac{r}{\rho z} + i\frac{\pi}{2}}. \quad (17)$$

Here we introduced $z = kr$. The integral is most easily calculated by deforming the integration contour so that it follows the positive half of the imaginary axis. The Hankel functions have a branching point at $z = 0$ and a cut that extends along the negative real axis. With such a choice of the branch cut the logarithm in the denominator takes the value $\ln(r/y\rho) - i\pi/2$ on the positive part of the imaginary axis ($z = iy$). The Hankel functions become Macdonald functions via $[H_i^{(1)}(iy)]^2 = \frac{4}{\pi^2}(-1)^{i+1}[K_i(y)]^2$. We therefore arrive at

$$n(r) = -\frac{4}{\pi^2 r\rho}\frac{J_0(g)}{J_1(g)}\int_0^\infty \frac{dy\left[K_0^2(y) - K_1^2(y)\right]}{\ln^2\left(\frac{r}{\rho y}\right) + \left(\frac{J_0(g)}{J_1(g)}\frac{r}{\rho y}\right)^2}. \quad (18)$$

Due to the exponentially suppressed Macdonald functions, this integral is dominated by $y \lesssim 1$. Then, unless the combination $J_0(g)/J_1(g)$ is small, the logarithm in the denominator can be safely neglected. Utilizing the numerical value of the integral, $\int_0^\infty dy y^2[K_0^2(y) - K_1^2(y)] = -\pi^2/16$, leads to the following expression:

$$n(r) = \frac{J_1(g)}{J_0(g)}\frac{\rho}{4r^3}. \quad (19)$$

This equation determines a nontrivial $g$ dependence, represented in Fig. 1. For weak impurities, $g \ll 1$, Eq. (19) reproduces the first Born approximation for the $\delta$ function (2), if one takes into account the obvious correspondence for the strength of the $\delta$ function, $\pi v g \rho \to U$. For strong impurities $g > 1$ the induced density is not positively defined and can become *negative*, which happens, for example, when $2.4 < g < 3.8$ (see Fig. 1).

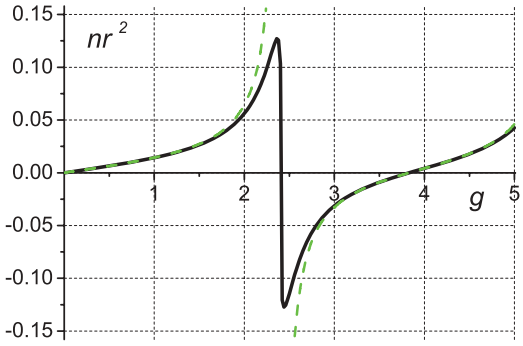


FIG. 1. (Color online) Dependence of the induced density (rescaled by $r^2$) on the dimensionless impurity strength, $g = V_0\rho/v$, plotted from Eq. (18) for $r/\rho = 10$. The approximation which is valid away from the resonance, Eq. (19), is shown for comparison with the green dashed line. The most notable feature is the reversal of the sign of the induced density from positive (electrons) to negative (holes) as $g$ passes through the point where $J_0(g) = 0$. Near the "antiresonance" point $g \approx 3.8$, determined by $J_1(g) = 0$, the impurity becomes "invisible" as the induced density is strongly suppressed by a small factor $\rho/r$.

When the impurity strength obeys the equation $J_1(g) = 0$, the induced density is strongly suppressed, e.g., for $g = 3.8$. In such a case it is no longer possible to use approximation (15). From Eq. (12) we now get $\gamma \approx k\rho(J_0/2 - J_1')$. The presence of an extra power of $k$ ensures much faster decay of the electron density:

$$n(r) \propto \frac{\rho^2}{r^4}. \quad (20)$$

So far we have discussed the contributions from the lowest-order $s$-wave scattering, $m = \pm 1/2$. A few words are now in order about higher $m$ channels. Equations (11) and (12) are fully applicable there as long as the order of the Bessel functions is adjusted: $0 \to m - 1/2$, $1 \to m + 1/2$ (for positive $m$). Instead of Eqs. (15) and (16) we now have $\gamma \propto (k\rho)^{m-1/2}$, $\beta \propto 1/(k\rho)^{m+1/2}$. From Eq. (13) we observe that each extra order of $m$ brings an additional factor $(k\rho)^2$. Upon taking the $k$ integral we conclude that already the $p$-wave scattering contribution is suppressed by a small factor $(\rho/r)^2$ and could be safely neglected. It is also known that for $|m| \geqslant 3/2$ zero energy bound states exist[20] when $J_{|m|-1/2}(V_0\rho) = 0$. However, as the electron density for these states decays $\propto r^{-2|m|-1}$ their contribution to $n(r)$ is negligible.

### A. The case of resonant scattering

With increasing $g$ the system passes through a set of resonances[21] determined by the condition $J_0(g_c) = 0$, the first of which occurs at $g_c = 2.4$ (Fig. 1). The physical origin of these resonances is quite clear and could be identified with the number of potential-induced Fermi wavelengths $v/V_0$ that fit inside the radius of the well, $\rho$. In the vicinity of the resonance, $J_0(g)$ in Eq. (18) could be expanded as

$$J_0(g) \approx -J_1(g_c)\delta g, \quad g = g_c + \delta g. \quad (21)$$

Contrary to the calculations of the preceding section, the logarithm in the denominator of Eq. (18) can no longer be

neglected. In fact the main contribution to the integral comes from small values of $y$. The numerator mostly comes from $K_1^2(y) \approx y^{-2}$, yielding

$$n(r) = -\frac{4\delta g}{\pi^2 r\rho}\int_0^1 \frac{dy}{y^2 \ln^2\left(\frac{r}{\rho y}\right) + \left(\delta g \frac{r}{\rho}\right)^2}. \quad (22)$$

In agreement with the assumption just made, the arguments relevant in integral (22) are small, $y \sim \delta g r/(\rho|\ln \delta g|) \ll 1$. With the logarithmic accuracy (neglecting double logarithm), we obtain

$$n(r) = \frac{2}{\pi r^2}\frac{\mathrm{sgn}(\delta g)}{\ln|\delta g|}, \quad |\delta g| \ll \frac{\rho}{r}\ln\left(\frac{r}{\rho}\right). \quad (23)$$

This relation describes the replacement of the growth of the density when a resonance is approached, see Eq. (19), with the ultimate logarithmic suppression in the immediate vicinity of it. The dependence of the density on distance changes from $r^{-3}$ away from the resonance to $r^{-2}$ near it. The maximum of the density occurs at impurity strength $|\delta g| \sim (\rho/r)\ln(r/\rho)$ where the two expressions (19) and (23) match, as could be expected. The behavior of the induced density in the vicinity of resonance is presented in Fig. 2.

It is now interesting to compute the total induced electron density. Such a calculation can be most rigorously carried out by integrating the general expression (18): it is convenient to first integrate over $r$ (from $\rho$ to $\infty$) and then over $y$. The same results, however, could be found much faster straight from Eqs. (19) and (23). Far from the resonance, $g \ll 1$, integrating Eq. (19) we obtain $N_{\mathrm{tot}} = \frac{\pi}{4}g$. As expected, in this perturbative regime the total disturbance of the system is small. Near the resonance, $\delta g \ll 1$, and upon integrating Eq. (23) from $\rho$ to $\rho/|\delta g|$ we arrive at

$$N_{\mathrm{tot}} = -4\mathrm{sgn}(\delta g). \quad (24)$$

Thus, the total number of particles induced by the resonant impurity is equal to *one per Dirac cone* (considering spin and valley degeneracy) and changes sign right at the resonance. This conclusion is in agreement with the Friedel sum rule.[2]

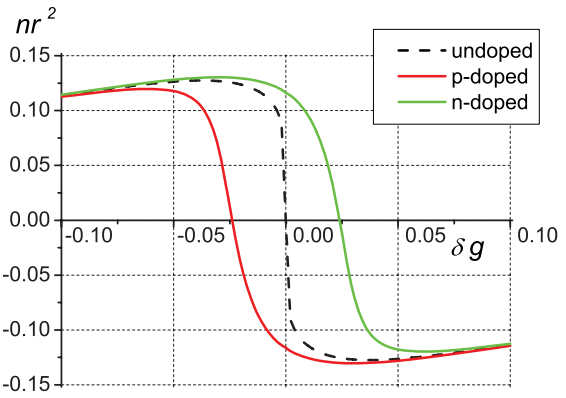


FIG. 2. (Color online) Sensitivity of the resonant behavior to small levels of doping, $k_F r = 0.05$, and $r/\rho = 10$. Induced density $n(r)r^2$ is plotted near $g = g_c + \delta g$. The black dashed line represents the behavior of induced density in undoped graphene. In the case of $p$ doping, the resonance is shifted by $\Delta g_c = k_F\rho\ln(k_F\rho) < 0$. Similarly, in the case of an $n$-doped system the changes are reversed (for the discussion of $n$-doped graphene see Sec. III C).

### B. $\delta$-function potential

We now discuss a connection between the finite-size well and the point impurity $V(\mathbf{r}) = U\delta(\mathbf{r})$. As already evident from Eq. (19), there is no rigorous limit of progressively narrower and higher potential, $g = V\rho/v \propto 1/\rho \to \infty$, as $\rho$ tends to zero. Alternatively, this could also be seen from the fact that the $\delta$-function potential does not allow a dimensionless coupling parameter independent of the distance $r$ of the kind that $g$ is for a finite-size well. Yet, there is a connection between the two models.

First we note that the combination of $\beta$ and $\gamma$ in the integrand of Eq. (14) is proportional to the $T$ matrix. Indeed, by taking the asymptotics of the wave function (11) the scattering phase shift could be expressed as $\tan\delta = -\gamma/\beta$. The relation between the phase $\delta$ and scattering amplitude in graphene is very similar to the standard quantum-mechanical expression[22] and was written in Ref. 18. In our notations,

$$T(k) = -\frac{4v}{k}\frac{\gamma}{\beta + i\gamma}. \quad (25)$$

Comparing now this general expression with Eq. (3) we can identify the phase shift for a point impurity,

$$\cot\delta = -\frac{\beta}{\gamma} = \frac{4v}{kU} - \frac{2}{\pi}\ln\left(\frac{1}{ka}\right). \quad (26)$$

From Eqs. (15) and (16) we can now extract the correspondence between the two problems,

$$U \longleftrightarrow 2\pi v\rho\frac{J_1(g)}{J_0(g)}. \quad (27)$$

The combination in the right-hand side (without $v$) could be identified with the scattering length of the circular potential well.[17]

We observe that the correspondence already encountered away from the resonances, cf. Eqs. (2) and (19), in fact holds everywhere. The finite-size resonances discussed in the previous section thus represent realizations of the unitary limit. Replacing now $\delta g \to -2\pi v\rho/U$ in Eq. (23) we arrive at Eq. (4) up to a replacement of $\rho$ with $a$ under the logarithm; this distinction is beyond logarithmic accuracy anyway.

It should be emphasized that the imaginary part in the scattering matrix Eq. (3) *cannot be neglected*. This can be seen following the transformation from Eq. (17) to Eq. (18), where it is important that the imaginary part is canceled by the phase coming from the logarithm upon the rotation to the imaginary axis. Without $i\pi/2$ in the denominator of Eq. (17), the density would have been finite in the unitary limit instead of the suppression described by Eq. (4).

Note that the correspondence (27) is different from what one would expect to be the true $\delta$-functional limit: $U \leftrightarrow \pi v g\rho$ with $\rho \to 0, g \to \infty$. Interestingly, the two models coincide with each other only in the case of a *shallow* well, $g \ll 1$. This situation is unique for the linear spectrum of graphene. Indeed, in the case of a conventional parabolic spectrum, $\epsilon = p^2/2m^*$, the dimensionless phase shift $\delta = \delta(V_0\rho^2 m^*)$ could only be a function of the combination $V_0\rho^2$ that becomes $U/\pi$ in the

limit of a deep and narrow well. This could be qualitatively understood by recalling that the parameter $Um^*$ gives the number of bound states in a well of depth $V_0 = U/\pi\rho^2$, which does not depend on $V_0$ or $\rho$ *separately*. In graphene, to the contrary, the phase shift is a function of $g = V_0\rho/v$.

Closely related to the $\delta$-function potential is the case of a pointlike Anderson impurity with a low-energy state $\varepsilon_0$ hybridized with graphene band electrons via $H_{\rm int} = u(d^\dagger\psi(0) + \text{c.c.})$, the problem considered in Ref. 14. When $\varepsilon_0 \approx 0$ the $T$ matrix has the resonant form (3) with the strength of the potential replaced by $U \to u^2/\varepsilon_0$. Similar substitution in Eq. (4) yields the distribution of the induced density. Note that the density is positive as long as $\varepsilon_0 > 0$ (electrons are expelled from the vicinity of the impurity) and negative when $\varepsilon_0 < 0$. Hydrogen adatoms are known to have resonances very close to the Dirac point,[23] $\varepsilon_0 \approx 30$ meV.

## III. EXTRINSIC GRAPHENE, $k_F \neq 0$

Let us now consider the case of gated or doped graphene with a nonzero Fermi momentum. We analyze two cases separately. When the distance to the impurity exceeds the Fermi wavelength, $k_F r \gg 1$, the conventional Friedel oscillations develop, whose specific behavior depends strongly on the impurity strength. The opposite case of a weakly gated graphene, $k_F r \ll 1$, is much more spectacular. Because of the resonant behavior described by Eqs. (4) and (19), the sensitivity of the induced density to small $k_F$ turns out to be very strong.

### A. Weakly *p*-doped or gated graphene, $k_F r \ll 1$

The case of a $p$-doped graphene is particularly straightforward as it is sufficient to simply replace the lower limit in the integral in Eq. (17) with $k_F r$. The integral is then written as $\int_0^\infty - \int_0^{k_F r}$, with the first one yielding the same expression as before, Eq. (4). The second integral brings the correction

$$\Delta n(r) = -\frac{2}{\pi r}\int_0^{k_F r} \frac{z\,dz}{\left[z\ln\left(\frac{r}{\rho z}\right) + \delta g\frac{r}{\rho}\right]^2 + \frac{\pi^2}{4}z^2}. \quad (28)$$

From the form of this integral it is clear that the correction is highly *asymmetric*: it quickly decays with increasing $\delta g$ when the latter is positive. For negative $\delta g < 0$ the correction (28) is much stronger because the integrand has a pole near the real axis. The pole is significant as long as $2k_F\rho\ln(k_F\rho) < \delta g < 0$. Outside of this region the correction again decreases quickly. This is illustrated in Fig. 2: the plot of the total density $n_{\rm tot}(r) = n(r) + \Delta n(r)$ is effectively "shifted" to the left of $g_c$. The first terms in the Taylor expansion in powers of $\delta g$ could be easily extracted:

$$n_{\rm tot}(r) = -\frac{2}{\pi r^2\ln(k_F\rho)}\left(1 + \frac{(\pi-2)\delta g}{k_F\rho\ln^2(k_F\rho)}\right). \quad (29)$$

The shift of the position of the resonance due to doping, $\Delta g_c$, with great precision is given by the condition $\beta(k_F) = 0$, yielding

$$\Delta g_c = -k_F\rho\ln\left(\frac{1}{k_F\rho}\right) \quad (30)$$

(see also discussion in the next section). Another consequence of Eq. (29) is that the singularity in the derivative of the undoped resonant density is regularized by finite $k_F$.

Let us emphasize the signature feature of the resonant behavior depicted in Fig. 2, namely the *reversal* of the sign of the density via small doping occurring in the range $\Delta g_c < \delta g < 0$.

#### 1. $\delta$-function potential

While the effects of weak doping lead to significant qualitative modification to the dependence of induced density on the distance for finite-size impurities, the corresponding changes for point defects are even more drastic. Note that the induced density in the latter case is *always* of the same sign as $U$ in the case of intrinsic graphene. In other words, the $\delta$-function potential roughly maps on the interval $0 < g < 2.4$, below the first resonance of the finite-size well, which corresponds to the $U \to \infty$ unitary limit; cf. Eq. (27). Doping with small amounts of holes (for $U > 0$) or electrons (for $U < 0$), on the other hand, *pushes* the resonance to a *finite* impurity strength $U_0$, so that for $U > U_0$ the induced particle density *changes* sign, much like in the case of a finite-size well. This strong modification of the induced density is captured in Fig. 3.

Although we explained following Eq. (27) that obtaining expressions for $U\delta(\mathbf{r})$ is rather simple, let us present here for reference the total induced density for the latter case,

$$n_{\rm tot}(r) = -\frac{8}{\pi r^2 u}\int_0^\infty dy \frac{K_0^2(y) - K_1^2(y)}{\ln^2\left(\frac{r}{ay}\right) + \left(\frac{2\pi}{uy}\right)^2} - \frac{2}{\pi r^2}\int_0^{k_F r}\frac{z\,dz}{\left[z\ln\left(\frac{r}{az}\right) - \frac{2\pi}{u}\right]^2 + \frac{\pi^2}{4}z^2}, \quad (31)$$

where by $u = U/vr$ we denoted the dimensionless parameter of the problem. Figure 3 illustrates the dependence of the

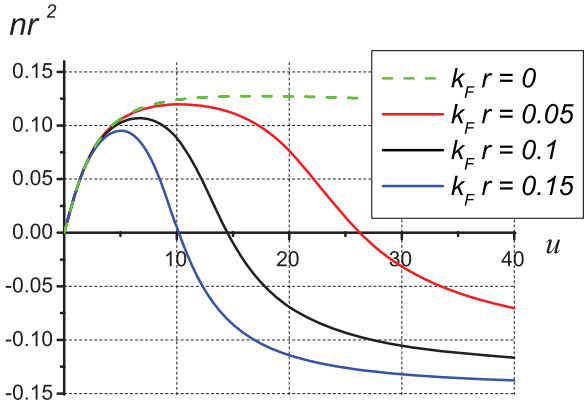


FIG. 3. (Color online) The emergence of a resonance for a pointlike impurity described by the $\delta$-function potential $V(r) = U\delta(\mathbf{r})$ for weak $p$-doping levels (for $U > 0$) vs the dimensionless impurity strength $u = U/vr$, plotted from Eq. (31), for $r/a = 10$. The green dashed line illustrates the undoped case: the logarithmic decay (4) is very weak on the scale shown. Finite $k_F$ makes the density change sign at $U_0$ given by Eq. (32). The same resonance is revealed via $n$ doping for an attractive potential of the impurity, $U < 0$.

induced density on $u$ for different values of doping levels $k_F r$. The density changes sign at the point where

$$U_0 = -\frac{2\pi v}{k_F \ln(k_F a)}. \tag{32}$$

At $U = U_0$ the scattering phase shift at the Fermi level $\delta_F$, determined by Eq. (25), undergoes a jump from $\pi/2$ to $-\pi/2$.

### B. Strongly *p*-doped case, $k_F r \gg 1$

With further increase in the doping level, the vicinity of the Fermi surface begins to dominate. Equation (14) with the lower limit replaced by $k_F r$ is a convenient starting point. Using the asymptotic expression $\sum_{i=0,1}[H_i^{(1)}(z)]^2 = -(\frac{2}{\pi z^2})\exp(2iz)$ and noting again that the ratio $\gamma/\beta = -\tan\delta$ is related to the phase shift $\delta$, we obtain

$$n(r) = \frac{4}{\pi^2 r^2}\mathrm{Im}\int_{k_F r}^{\infty}\frac{dz}{z}\sin\delta e^{2iz+i\delta}. \tag{33}$$

Because of the strongly oscillating behavior of the integrand only the vicinity of the lower limit contributes to the density. After simple integration we arrive at

$$n(r) = 2\sin\delta_F\frac{\cos(2k_F r+\delta_F)}{\pi^2 k_F r^3}, \tag{34}$$

with the scattering phase shift taken at the Fermi surface, $\delta_F = -\tan^{-1}[\gamma(k_F)/\beta(k_F)]$. The formula (34) describes Friedel oscillations both in the perturbative limit, where $\delta_F \ll 1$ and Eq. (1) is recovered, and in the resonant (unitary) regime, when $\delta_F$ is close to $\pm\pi/2$, where the amplitude of the oscillations no longer depends on the impurity strength. Note that in the vicinity of the resonance the density (34) reverses its sign, similar to the intrinsic case.

### C. *n*-doped graphene

Now we discuss $n$-doped graphene with a ground state filled up to a positive Fermi energy, $E_F > 0$. According to our notation, $k = -E/v$, in the $n$-doped case the range of positive energies with $k_F < k < 0$ appears in addition to the filled lower Dirac cone. For negative $k$ the eigenfunctions Eq. (11) are still applicable with coefficients now assuming the form

$$\begin{aligned}\beta &= J_1(k\rho+g)Y_0(|k|\rho)+J_0(k\rho+g)Y_1(|k|\rho),\\ \gamma &= -J_0(k\rho+g)J_1(|k|\rho)-J_1(k\rho+g)J_0(|k|\rho),\end{aligned} \tag{35}$$

implying that Eq. (15) holds for $\gamma$ with both signs of $k$, whereas Eq. (16) captures correct $\beta$ for all values of $k$ if one changes $k$ to $|k|$ in the argument of logarithm. Taking this into account, the induced density is given by Eq. (13) or Eq. (14), provided that the lower limit of the integral is extended to $k_F$ and $k$ is changed to $|k|$ in the rest of the integrand. We write it as

$$n(r) = \frac{2}{\pi}\mathrm{Im}\sum_{i=0,1}\left\{\int_{-\infty}^{\infty}-\int_{-\infty}^{-|k_F|}\right\}\frac{dk\,|k|\gamma}{\beta+i\gamma}\left[H_i^{(1)}(|k|r)\right]^2. \tag{36}$$

It is straightforward to check that the first integral here is zero. Indeed, as a combination of integrals over $(-\infty, 0)$ and $(0, \infty)$, it amounts to the sum of two integrals, one of which is the same as in Eq. (17), while the other one is given by Eq. (17) with the opposite sign of $J_0(g)/J_1(g)$ in the denominator. According to Eq. (18) such a combination is zero.

We conclude that the induced density is governed by the second integral of Eq. (36), leading to relation (34) with the opposite sign. Therefore, the general relation for induced density (Friedel oscillations) in strongly doped graphene is

$$n(r) = -\frac{2v\sin\delta_F}{E_F}\frac{\cos(2|k_F|r+\delta_F)}{\pi^2 r^3}. \tag{37}$$

The phase shift at the Fermi surface is determined by [cf. Eq. (26)]

$$\cot\delta_F = -\frac{2v}{\pi E_F\rho}\frac{J_0(g)}{J_1(g)}-\frac{2}{\pi}\ln\left(\frac{v}{|E_F|\rho}\right). \tag{38}$$

Expression (37) generalizes Eq. (1) and has the latter as the limiting case at weak couplings. The long behavior is always $\propto r^{-3}$, even at resonance, as opposed to the intrinsic graphene, Eq. (4). Still, as one passes through a resonance, the phase shift jumps by $\pi$ and the sign of the induced density reverses, much like in Fig. 1.

## IV. SUMMARY AND CONCLUSIONS

In this paper we considered the two nonperturbative models for impurities in graphene: a substitution atom described by $V(\mathbf{r}) = U\delta(\mathbf{r})$, and a finite-size impurity (molecule or nanoparticle) with $V(\mathbf{r}) = V_0\Theta(\rho - r)$. The first model cannot be derived from the second one via a standard limiting procedure in the effective low-energy Dirac fermion description, although there is a simple correspondence between the two. As an illustration of the scattering problem we calculated the impurity-induced density for both intrinsic and extrinsic (doped) graphene.

The case of a finite-size potential reveals a set of resonances that correspond to the zeros of the Bessel function, $J_0(g) = 0$, for the dimensionless impurity strength, $g = V_0\rho/v$ (see Fig. 1). Near a resonance (which is an effective realization of the unitary limit) the $r^{-3}$ decay of the induced density is replaced with a slower $r^{-2}$ dependence. The resonances are interspaced with "antiresonances" that occur when $J_1(g) = 0$. At the latter points the induced density becomes strongly suppressed with the long-distance behavior $\propto r^{-4}$. Low dopings, $k_F r \ll 1$, modify the vicinity of resonances leading to the shift of the resonant coupling $g_c$ and removal of the logarithmic singularity, Fig. 2. The rest of the $n(g,r)$ dependence is unaffected by low $k_F$, including positions of the antiresonances. At stronger doping levels, $k_F r \gg 1$, the induced density follows the usual Friedel $\cos(2k_F r)/r^3$ dependence known from the first Born approximation, with the resonant behavior entering via the phase shifts. In particular, near the resonances the induced density reverses sign. The Friedel oscillations remain strongly suppressed near antiresonances.

The point impurity model $V = U\delta(\mathbf{r})$ does not have antiresonances. In the intrinsic case the only true resonance occurs at $U = \infty$, though the maximum of the induced density is found near $U \sim 10vr$. With the doping the resonance is shifted to the finite values $U_0$ given by Eq. (32) (see Fig. 3).

Our findings indicate that the unitary limit of strong impurities could be realized with realistic potentials $V_0$. In particular, for a nanometer-size impurity $\rho \approx 1$ nm the first resonance occurs when $V_0 = 2.4v\hbar/\rho \approx 1.5$ eV. Correspondingly, for an extended $\rho \approx 10$ nm defect the potential would have to be only $V_0 \approx 150$ meV.

## ACKNOWLEDGMENTS

Useful discussions with M. Raikh, O. Starykh, and P. G. Silvestrov are gratefully acknowledged. The work was supported by the Department of Energy, Office of Basic Energy Sciences, Grant No. DE-FG02-06ER46313.

*vmkhitar@gmail.com

[1] D. Pines and P. Nozieres, *The Theory of Quantum Liquids* (Benjamin, New York, 1966).
[2] J. Friedel, Philos. Mag. **43**, 153 (1952).
[3] K. H. Lau and W. Kohn, Surf. Sci. **75**, 69 (1978).
[4] G.-H. Chen and M. E. Raikh, Phys. Rev. B **60**, 4826 (1999).
[5] A. H. Castro Neto, F. Guinea, N. M. R. Peres, K. S. Novoselov, and A. K. Geim, Rev. Mod. Phys. **81**, 109 (2009).
[6] V. V. Cheianov and V. I. Fal'ko, Phys. Rev. Lett. **97**, 226801 (2006).
[7] Á. Bácsi and A. Virosztek, Phys. Rev. B **82**, 193405 (2010).
[8] P. M. Ostrovsky, I. V. Gornyi, and A. D. Mirlin, Phys. Rev. B **74**, 235443 (2006).
[9] N. M. R. Peres, F. Guinea, and A. H. Castro Neto, Phys. Rev. B **73**, 125411 (2006).
[10] T. Stauber, N. M. R. Peres, and F. Guinea, Phys. Rev. B **76**, 205423 (2007).
[11] A. V. Shytov, D. A. Abanin, and L. S. Levitov, Phys. Rev. Lett. **103**, 016806 (2009).
[12] C. Bena and S. A. Kivelson, Phys. Rev. B **72**, 125432 (2005).
[13] D. M. Basko, Phys. Rev. B **78**, 115432 (2008).
[14] T. O. Wehling, M. I. Katsnelson, and A. I. Lichtenstein, Chem. Phys. Lett. **476**, 125 (2009).
[15] N. M. R. Peres, F. Guinea, and A. H. Castro Neto, Phys. Rev. B **73**, 125411 (2006).
[16] M. Hentschel and F. Guinea, Phys. Rev. B **76**, 115407 (2007).
[17] M. Titov, P. M. Ostrovsky, I. V. Gornyi, A. Schuessler, and A. D. Mirlin, Phys. Rev. Lett. **104**, 076802 (2010).
[18] D. S. Novikov, Phys. Rev. B **76**, 245435 (2007).
[19] We normalize the wave functions on the "$k/2\pi$ scale," $\int drr[\varphi^*_{1k}(r)\varphi_{1k'}(r) + \varphi^*_{2k}(r)\varphi_{2k'}(r)] = 2\pi\delta(k-k')$.
[20] J. H. Bardarson, M. Titov, and P. W. Brouwer, Phys. Rev. Lett. **102**, 226803 (2009); M. Schneider and P. W. Brouwer, Phys. Rev. B **84**, 115440 (2011).
[21] Resonances that occur without formation of bound states were previously studied in gapless semiconductors within Luttinger Hamiltonian by N. N. Ablyazov, B. L. Gel'mont, M. E. Raikh, and A. L. Efros, Zh. Eksp. Teor. Fiz. **87**, 646 (1984) [Sov. Phys. JETP **60**, 371 (1984)].
[22] L. D. Landau and E. M. Lifshitz, *Quantum Mechanics: Non-Relativistic Theory* (Addison-Wesley, Reading, MA, 1958).
[23] T. O. Wehling, M. I. Katsnelson, and A. I. Lichtenstein, Phys. Rev. B **80**, 085428 (2009).